X CONGRESSO NACIONAL DE ENGENHARIA MECÂNICA 2018
ABCM
20 A 24 DE MAIO DE 2018 SALVADOR – BA – BRASIL

TOWARDS A DYNAMIC ITERATIVE COUPLING SCHEME APPLIED TO THE TRANSIENT RESPONSE OF RIGID FOUNDATIONS INTERACTING WITH SOIL PROFILES

Otávio Augusto Tovo, otaviotovo@hotmail.com[1]
Luis Filipe do Vale Lima, lfvlima@fem.unicamp.br[1]
Daniela Andrade Damasceno, daniela@fem.unicamp.br[1]
Josué Labaki, labaki@fem.unicamp.br[2]
Euclides de Mesquita Neto, euclides@fem.unicamp.br[1]

[1] Department of Computational Mechanics, School of Mechanical Engineering, University of Campinas, 200 Mendeleyev Street, 13083-970, Campinas, São Paulo, Brazil.
[2] Department of Integrated Systems, School of Mechanical Engineering, University of Campinas, 200 Mendeleyev Street, 13083-970, Campinas, São Paulo, Brazil.

Abstract: *This article describes an iterative coupling scheme to analyze the transient dynamic response of structures interacting with distinct soil profiles. Structures with lumped parameters and linear equations of motions are solved by the Newmark integration scheme. The soil, on the other hand, is an unbounded domain presenting outgoing and non-reflected waves that withdraw energy from the excitation source. This effect is known as Sommerfeld radiation condition or radiation damping. The modeling of unbounded domains presenting radiation damping requires special techniques that incorporate this damping effect, such as the Boundary Element Method (BEM) or a semi-analytical method based on a Green's function approach (GF). The stationary dynamic behavior of soils have been successfully solve by the BEM and GF strategies. Nevertheless, the transient dynamic response of structures interacting with unbounded domains is still limited to a few cases. In this article the stationary dynamic response of the soil has been obtained by GF methods for very high frequencies, which, in conjunction with the FFT algorithm, allows to obtain accurate soil impulse responses for small time steps. The soil response to arbitrary transient excitation is obtained by Duhamel's convolution integral. Previous research results indicate that the iterative coupling scheme is highly dependent on the accuracy of the strategies applied to solve each subsystem. The convergence rate of the convoluiton integral with constant time interpolation is smaller than the one presented by the Newmark algorithm. This convergence rate discrepancy causes convergence failure in the iterative scheme. The present article describes a formulation and an implementation of a convolution integral with higher order time interpolation schemes, which is essential to improve the convergence properties of the proposed iterative scheme. This higher order convolution integrals are essential steps to formulate a robust iterative algorithm to determine the transient response of coupled soil-structure systems. The convergence rates of the proposed convolution integrals are compared with those of the classical Newmark algorithm.*

Keywords: *Dynamic Soil Structure Interaction, Transient foundation response, Iterative coupling procedure, Higher order Duhamel convolution integral.*

1. INTRODUCTION

This article describes an iterative coupling scheme to analyze the transient dynamic response of structures interacting with distinct soil profiles. Structures with lumped parameters and linear equations of motions are considered. These time domain linear equations are solved by the Newmark integration scheme. The soil, on the other hand, is an unbounded domain presenting outgoing and non-reflecting waves that withdraw energy from the excitation source. This effect is known as Sommerfeld radiation condition or radiation damping. The modeling of unbounded domains presenting radiation damping requires special techniques that incorporate this damping effect, such as the Boundary Element Method (BEM) (Carrion *et al.*, 2007) or a semi-analytical method based on a Green's function approach (GF) (Labaki *et al.*, 2014). The stationary dynamic behavior of soils has been successfully solved by the BEM and GF strategies (Carrion *et al.*, 2007; Labaki *et al.*, 2014). The transient analysis of phenomena modelled by the BEM has experienced large progress as can be seen in the literature (Coda and Venturini, 1995; Gaul *et al.*, 1992). Nevertheless, the transient dynamic response of structures interacting with unbounded domains is still limited to a few cases. This article

aims to describe an iterative coupling strategy that allows to obtain the transient solution of linear structures interacting with unbounded soil profiles. The stationary dynamic response of the soil has been obtained for very high frequencies, which, in conjunction with the FFT algorithm, allows to obtain soil impulse responses very accurately and for very small steps (Mesquita *et al.*, 2012). The soil response to arbitrary time excitation is obtained by a convolution integral, Duhamel's integral (Mesquita *et al.*, 2012; Damasceno, 2013). Special attention is given to higher order implementation of the Duhamel's integration scheme, which is a requirement to achieve accurate results for the soil response.

2. STATEMENT OF PROBLEM

A very attractive scheme to determine the transient response of foundations and structures interacting with the soil is given by an iterative coupling of the subsystems. This is exemplified in Fig. (1). A foundation of mass, M_f, is interacting with an unbounded soil domain of Lamé constant G, mass density ρ, and material damping η. The system is excited by an external, transient force F_{ext}. Soil and foundation may be considered as two distinct systems and each separate system can be solved by the best available methodology. At the interface between the systems interface forces $F_{S1} = F_{S2}$ are observed. The displacement of the interface is U_F and U_S. The transient response of the foundation may be determined by a time integration algorithm, i.e., the Newmark integration scheme. The transient response of the soil may be obtained by performing a convolution between the current excitation F_{S2} and the response due to unit pulse excitation, also called transient Green's function. A typical example of a soil response to a unit impulse is shown in Fig. (2) (Mesquita *et al.*, 2012), in which an axisymmetric circular vertical impulse of radius *a* is applied at the surface of a homogeneous half-space. The resulting vertical displacement $u_{zz}(t)$ of a point within the half-space is shown in the figure, where wave fronts due to pressure (P), shear (S) and Rayleigh (R) waves arrive at the observation point at times t_P, t_S and t_R, respectively.

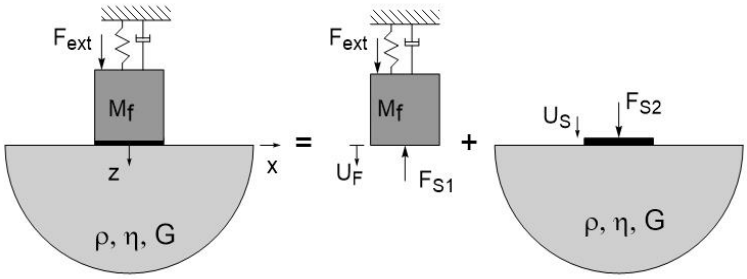

Figure 1. Decomposition of soil-foundation into two subsystems.

The proposed strategy is to couple iteratively two subsystems, the response of the first, the structure, being determined by a classical time integration algorithm and the soil response by a convolution integral. This scheme has been implemented by Damasceno (2013) and Damasceno *et al.*, (2013). One of the findings of that research is that the convergence of the iterative coupling procedure is highly dependent on the accuracy of the solution scheme used for each subsystem. In the work of Damasceno (2013), the Newmark integration scheme and a convolution with constant time interpolation was used.

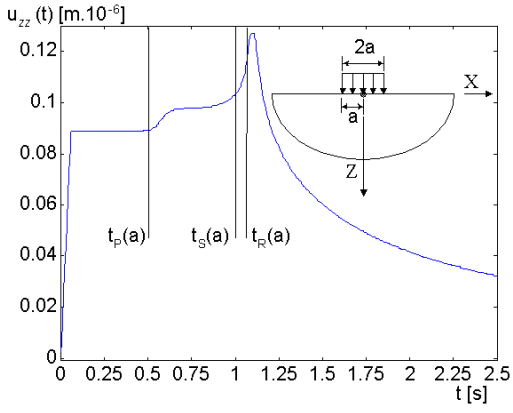

Figure 2. Typical transient soil response to a unit impulse force.

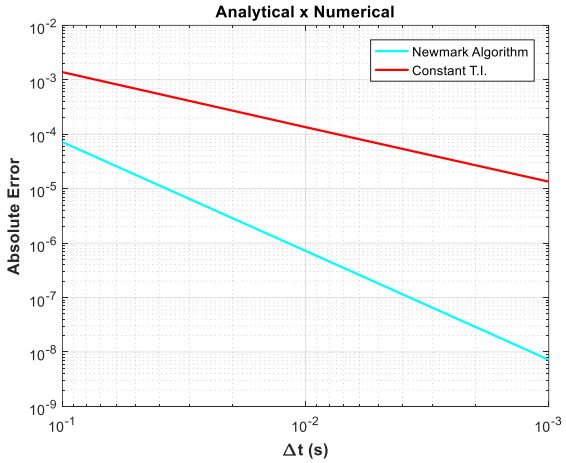

Figure 3. Convergence of error between analytical and numerical solution.

Figure (3) shows the convergence rate, with respect to the length of the time step, for the Newmark algorithm and for the convolution integral with constant time interpolation. One can recognize that the Newmark convergence rate is 2 but on the other hand the convergence for the 'constant time interpolation' convolution is only 1. The iterative scheme fails frequently due to this mismatch in the convergence rates.

3. PROPOSED SOLUTION

In the present article, a formulation and an implementation of a convolution integral with linear and quadratic time interpolation strategy is described. The convergence rate of these higher order convolution integrals is compared with the constant time interpolation and the Newmark algorithm. It will be shown that the higher order convolution integral has a higher convergence rate and may represent a significant improvement for the soil-foundation iterative coupling scheme.

4. FORMULATION

4.1. Analytical Convolution Integral

According to Cheng (1972), the transient response for a linear system can be obtained from the convolution integral shown in Eq. (1) below:

$$c(t_{max}) = \int_{\tau=0}^{\tau=t_{max}} f(\tau).h(t_{max} - \tau)\, d\tau \tag{1}$$

4.2. Numerical convolution integral approximated by first order (linear) shape functions

Considering the example assuming that $t_{max} = 2\Delta t$, that is, only the two initial time steps determined:

$$c(t_{max} = 2\Delta t) = \int_{\tau=0}^{\tau=2\Delta t} f(\tau).h(2\Delta t - \tau)\, d\tau = \underbrace{\int_{\tau=0}^{\tau=\Delta t} f(\tau).h(t_{max} - \tau)\, d\tau}_{c_1(t_{max}=2\Delta t)} + \underbrace{\int_{\tau=\Delta t}^{\tau=2\Delta t} f(\tau).h(t_{max} - \tau)\, d\tau}_{c_2(t_{max}=2\Delta t)} \tag{2}$$

As shown in Eq. (2), the first integration interval is $0 \le \tau \le \Delta t$. Thus, $c_1(t_{max} = 2\Delta t)$ is written by:

$$c_1(t_{máx} = 2\Delta t) = \int_{\tau=0}^{\tau=\Delta t} f(\tau).h(2\Delta t - \tau)\, d\tau \tag{3}$$

In Eq. (3), f (τ) can be approximated by first order shape functions. Thus, in Eq. (4), N_1 (τ) and N_2 (τ) are first order shape functions developed by the Lagrange Theorem, and it is given by:

$$f(\tau) = f_1.N_1(\tau) + f_2.N_2(\tau) \tag{4}$$

In Eq. (3), h (t_{max} - τ) can be approximated by first order shape functions. Thus, in Eq. (5), N_1 (t_{max} - τ) and N_2 (t_{max} - τ) are first order shape functions developed by the Lagrange Theorem, and it is given by:

$$h(t_{max} - \tau) = h_2.N_1(t_{max} - \tau) + h_3.N_2(t_{max} - \tau) \tag{5}$$

Substituting Eq. (4) and Eq. (5) into Eq. (3) yields:

$$c_1(t_{máx} = 2\Delta t) = \int_{\tau=0}^{\tau=\Delta t} \left[f_1.N_1(\tau) + f_2.N_2(\tau)\right].\left[h_2.N_1(t_{máx} - \tau) + h_3.N_2(t_{máx} - \tau)\right] d\tau \tag{6}$$

Analogously, as shown in Eq. (2), the second integration interval is $\Delta t \le \tau \le 2\Delta t$. Thus, $c_2(t_{max} = 2\Delta t)$ is written as:

$$c_2(t_{máx} = 2\Delta t) = \int_{\tau=\Delta t}^{\tau=2\Delta t} f(\tau).h(2\Delta t - \tau)\, d\tau \tag{7}$$

Equation (7) approximated by first order shape functions is given by:

$$c_2(t_{máx} = 2\Delta t) = \int_{\tau=\Delta t}^{\tau=2\Delta t} \left[f_2.N_1(\tau) + f_3.N_2(\tau)\right].\left[h_1.N_1(t_{máx} - \tau) + h_2.N_2(t_{máx} - \tau)\right] d\tau \quad (8)$$

Note that in Eq. (8) the subscripts of 'f' and 'h' are different from Eq. (6), because now the integration interval is $\Delta t \leq \tau \leq 2\Delta t$.

The process of numerical approximation used in Eq. (6) and Eq. (8) is illustrated below:

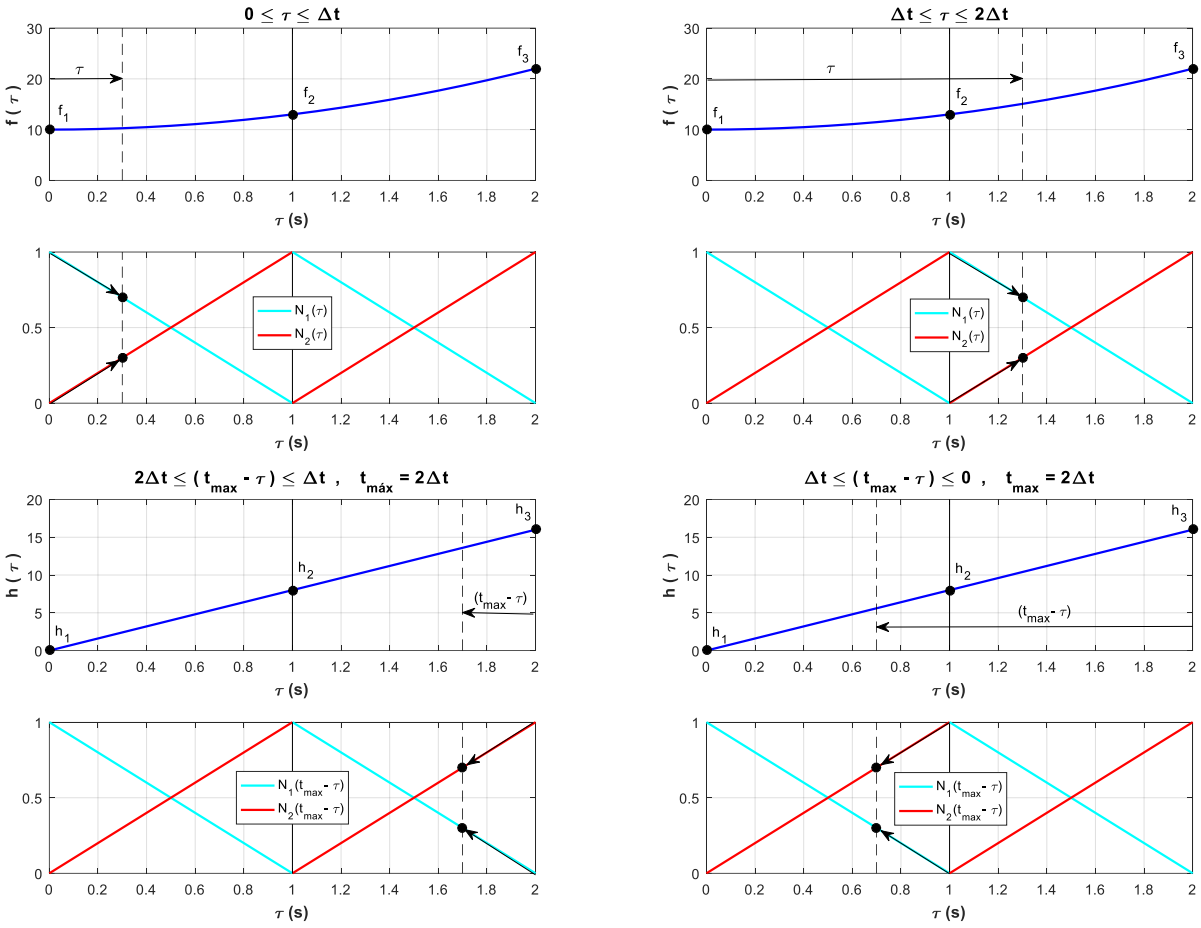

Figure 4. Numerical convolution integral $c_1(t_{max}=2\Delta t)$. (b) Numerical convolution integral $c_2(t_{max}=2\Delta t)$.

Now, the goal is to manipulate algebraically Eq. (6) to obtain integral expressions which can be solved numerically. Thus, applying distributive property and manipulating the terms in Eq. (6) one can obtain Eq. (9), which is written in matrix form as:

$$c_1(t_{máx} = 2\Delta t) = \left\{ \begin{bmatrix} f_1 & f_2 \end{bmatrix}_{1x2} . \begin{bmatrix} \int_{\tau=0}^{\tau=\Delta t} N_1(\tau).N_1(t_{máx} - \tau) d\tau & \int_{\tau=0}^{\tau=\Delta t} N_1(\tau).N_2(t_{máx} - \tau) d\tau \\ \int_{\tau=0}^{\tau=\Delta t} N_2(\tau).N_1(t_{máx} - \tau) d\tau & \int_{\tau=0}^{\tau=\Delta t} N_2(\tau).N_2(t_{máx} - \tau) d\tau \end{bmatrix}_{2x2} . \begin{bmatrix} h_2 \\ h_3 \end{bmatrix}_{2x1} \right\} . \Delta t \quad (9)$$

Solving numerically the integral expressions in Eq. (9) and rewriting:

$$c_1(t_{max} = 2\Delta t) = \left\{ \begin{bmatrix} f_1 & f_2 \end{bmatrix}_{1x2} . \begin{bmatrix} \left(\frac{1}{6}\right) & \left(\frac{1}{3}\right) \\ \left(\frac{1}{3}\right) & \left(\frac{1}{6}\right) \end{bmatrix}_{2x2} . \begin{bmatrix} h_2 \\ h_3 \end{bmatrix}_{2x1} \right\} . \Delta t \quad (10)$$

The manipulation for Eq. (8) is the same applied in Eq. (6), thus:

$$c_2(t_{máx}=2\Delta t)=\left\{\begin{bmatrix}f_2 & f_3\end{bmatrix}_{1x2}.\begin{bmatrix}\int_{\tau=\Delta t}^{\tau=2\Delta t}N_1(\tau).N_1(t_{máx}-\tau)d\tau & \int_{\tau=\Delta t}^{\tau=2\Delta t}N_1(\tau).N_2(t_{máx}-\tau)d\tau\\ \int_{\tau=\Delta t}^{\tau=2\Delta t}N_2(\tau).N_1(t_{máx}-\tau)d\tau & \int_{\tau=\Delta t}^{\tau=2\Delta t}N_2(\tau).N_2(t_{máx}-\tau)d\tau\end{bmatrix}_{2x2}.\begin{bmatrix}h_1\\h_2\end{bmatrix}_{2x1}\right\}.\Delta t \quad (11)$$

Solving numerically the integral expressions in Eq. (11):

$$c_2(t_{max}=2\Delta t)=\left\{\begin{bmatrix}f_2 & f_3\end{bmatrix}_{1x2}.\begin{bmatrix}\left(\frac{1}{6}\right) & \left(\frac{1}{3}\right)\\ \left(\frac{1}{3}\right) & \left(\frac{1}{6}\right)\end{bmatrix}_{2x2}.\begin{bmatrix}h_1\\h_2\end{bmatrix}_{2x1}\right\}.\Delta t \quad (12)$$

Therefore, substituting Eq. (10) and Eq. (12) into Eq. (2), yields:

$$c(t_{max}=2\Delta t)=\left\{\underbrace{\begin{bmatrix}f_1 & f_2\end{bmatrix}_{1x2}.\begin{bmatrix}\left(\frac{1}{6}\right) & \left(\frac{1}{3}\right)\\ \left(\frac{1}{3}\right) & \left(\frac{1}{6}\right)\end{bmatrix}_{2x2}.\begin{bmatrix}h_2\\h_3\end{bmatrix}_{2x1}}_{c_1(t_{max}=2\Delta t)}+\underbrace{\begin{bmatrix}f_2 & f_3\end{bmatrix}_{1x2}.\begin{bmatrix}\left(\frac{1}{6}\right) & \left(\frac{1}{3}\right)\\ \left(\frac{1}{3}\right) & \left(\frac{1}{6}\right)\end{bmatrix}_{2x2}.\begin{bmatrix}h_1\\h_2\end{bmatrix}_{2x1}}_{c_2(t_{max}=2\Delta t)}\right\}.\Delta t \quad (13)$$

One cans possible generalize Eq. (13) for the interval $0 \le \tau \le n\Delta t$:

$$c(t_{máx}=n\Delta t)=\sum_{i=1}^{n}\left\{\begin{bmatrix}f_{(i)} & f_{(i+1)}\end{bmatrix}_{1x2}.\begin{bmatrix}\left(\frac{1}{6}\right) & \left(\frac{2}{6}\right)\\ \left(\frac{2}{6}\right) & \left(\frac{1}{6}\right)\end{bmatrix}_{2x2}.\begin{bmatrix}h_{((n-i)+1)}\\h_{((n-i)+2)}\end{bmatrix}_{2x1}\right\}.\Delta t \quad (14)$$

4.3. Numerical convolution integral approximated by second order (quadratic) shape functions

Considering the same example used in Eq. (2). In Eq. (3), f (τ) can be approximated by second order shape functions. Thus, in Eq. (15), N_1 (τ), N_2 (τ) and N_3 (τ) are second order shape functions developed by the Lagrange Theorem, and it is given by:

$$f(\tau)=f_1.N_1(\tau)+f_2.N_2(\tau)+f_3.N_3(\tau) \quad (15)$$

In Eq. (3), h (t_{max} - τ) can be approximated by second order shape functions. Thus, in Eq. (15), N_1 (t_{max} - τ), N_2 (t_{max} - τ) and N_3 (t_{max} - τ) are second order shape functions developed by the Lagrange Theorem:

$$h(t_{max}-\tau)=h_1.N_1(t_{max}-\tau)+h_2.N_2(t_{max}-\tau)+h_3.N_3(t_{max}-\tau) \quad (16)$$

Substituting Eq. (15) and Eq. (16) into Eq. (3) yields:

$$c_1(t_{max}=2\Delta t)=\int_{\tau=0}^{\tau=\Delta t}\left[f_1.N_1(\tau)+f_2.N_2(\tau)+f_3.N_3(\tau)\right].\left[h_1.N_1(t_{max}-\tau)+h_2.N_2(t_{max}-\tau)+h_3.N_3(t_{max}-\tau)\right]d\tau \quad (17)$$

Equation (7) approximated by second order shape functions is given by:

$$c_2(t_{max}=2\Delta t)=\int_{\tau=\Delta t}^{\tau=2\Delta t}\left[f_1.N_1(\tau)+f_2.N_2(\tau)+f_3.N_3(\tau)\right].\left[h_1.N_1(t_{max}-\tau)+h_2.N_2(t_{max}-\tau)+h_3.N_3(t_{max}-\tau)\right]d\tau \quad (18)$$

The process of numerical approximation used in Eq. (17) and Eq. (18) is illustrated below:

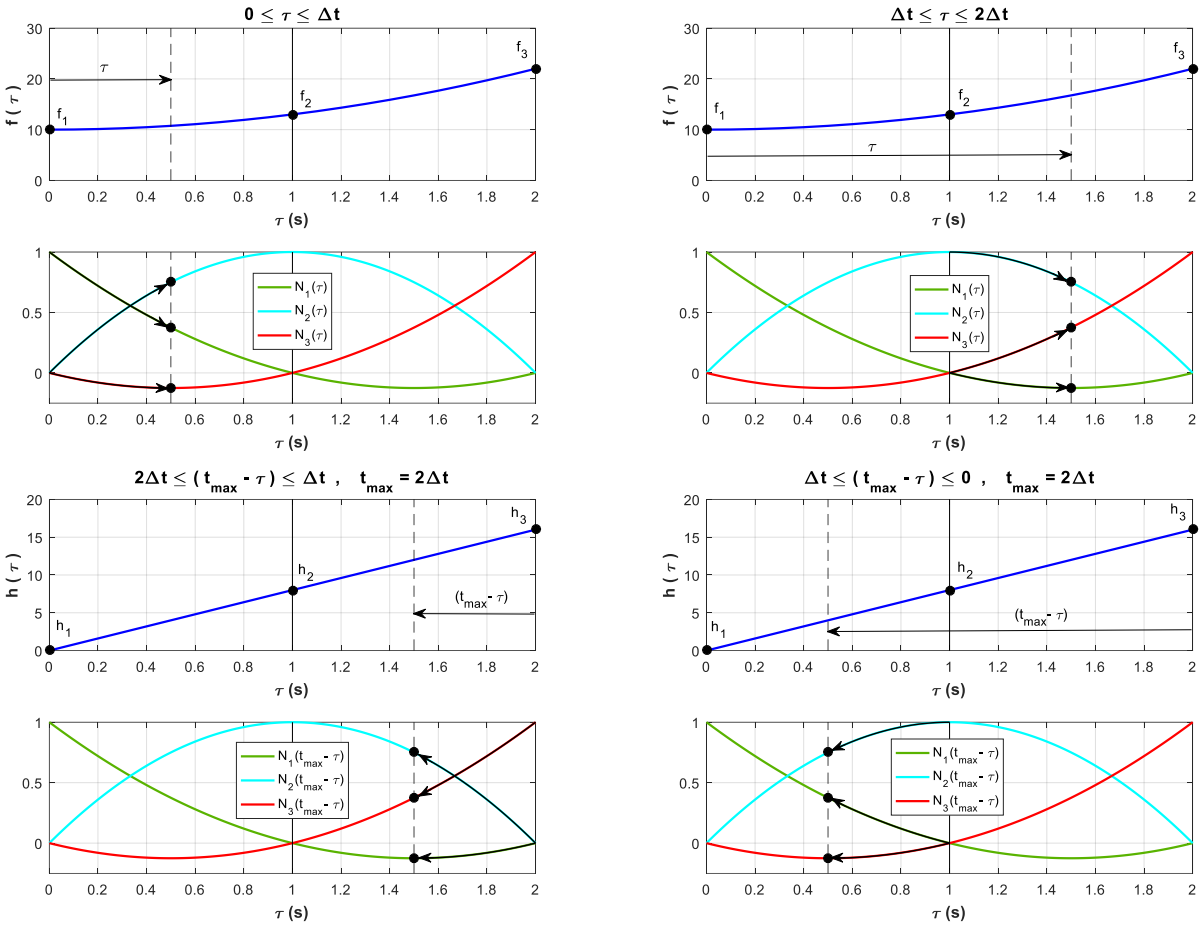

(a) (b)

Figure 5. (a) Numerical convolution integral $c_1(t_{max}=2\Delta t)$. (b) Numerical convolution integral $c_2(t_{max}=2\Delta t)$.

Now, the goal is to manipulate algebraically Eq. (17) to obtain integral expressions which can be solved numerically. Thus, applying distributive property and manipulating the terms in Eq. (17) one can obtain Eq. (19), which is written in matrix form:

$$c_1 = \left\{ \begin{bmatrix} f_1 \\ f_2 \\ f_3 \end{bmatrix}^T_{3x1} . \begin{bmatrix} \int_{\tau=0}^{\tau=\Delta t} N_1(\tau).N_1(t_{máx}-\tau)\,d\tau & \int_{\tau=0}^{\tau=\Delta t} N_1(\tau).N_2(t_{máx}-\tau)\,d\tau & \int_{\tau=0}^{\tau=\Delta t} N_1(\tau).N_3(t_{máx}-\tau)\,d\tau \\ \int_{\tau=0}^{\tau=\Delta t} N_2(\tau).N_1(t_{máx}-\tau)\,d\tau & \int_{\tau=0}^{\tau=\Delta t} N_2(\tau).N_2(t_{máx}-\tau)\,d\tau & \int_{\tau=0}^{\tau=\Delta t} N_2(\tau).N_3(t_{máx}-\tau)\,d\tau \\ \int_{\tau=0}^{\tau=\Delta t} N_3(\tau).N_1(t_{máx}-\tau)\,d\tau & \int_{\tau=0}^{\tau=\Delta t} N_3(\tau).N_2(t_{máx}-\tau)\,d\tau & \int_{\tau=0}^{\tau=\Delta t} N_3(\tau).N_3(t_{máx}-\tau)\,d\tau \end{bmatrix}_{3x3} . \begin{bmatrix} h_1 \\ h_2 \\ h_3 \end{bmatrix}_{3x1} \right\} .\Delta t \quad (19)$$

Solving numerically the integral expressions in Eq. (19):

$$c_1 = \left\{ \begin{bmatrix} f_1 \\ f_2 \\ f_3 \end{bmatrix}^T_{3x1} . \begin{bmatrix} \left(-\frac{4}{120}\right) & \left(\frac{23}{120}\right) & \left(\frac{31}{120}\right) \\ \left(-\frac{7}{120}\right) & \left(\frac{64}{120}\right) & \left(\frac{23}{120}\right) \\ \left(\frac{1}{120}\right) & \left(-\frac{7}{120}\right) & \left(-\frac{4}{120}\right) \end{bmatrix}_{3x3} . \begin{bmatrix} h_1 \\ h_2 \\ h_3 \end{bmatrix}_{3x1} \right\} .\Delta t \quad (20)$$

The manipulation for Eq. (18) is the same applied in Eq. (17), thus:

$$c_2 = \left\{ \begin{bmatrix} f_1 \\ f_2 \\ f_3 \end{bmatrix}_{3x1}^T . \begin{bmatrix} \int_{\tau=\Delta t}^{\tau=2\Delta t} N_1(\tau).N_1(t_{máx}-\tau)d\tau & \int_{\tau=\Delta t}^{\tau=2\Delta t} N_1(\tau).N_2(t_{máx}-\tau)d\tau & \int_{\tau=\Delta t}^{\tau=2\Delta t} N_1(\tau).N_3(t_{máx}-\tau)d\tau \\ \int_{\tau=\Delta t}^{\tau=2\Delta t} N_2(\tau).N_1(t_{máx}-\tau)d\tau & \int_{\tau=\Delta t}^{\tau=2\Delta t} N_2(\tau).N_2(t_{máx}-\tau)d\tau & \int_{\tau=\Delta t}^{\tau=2\Delta t} N_2(\tau).N_3(t_{máx}-\tau)d\tau \\ \int_{\tau=\Delta t}^{\tau=2\Delta t} N_3(\tau).N_1(t_{máx}-\tau)d\tau & \int_{\tau=\Delta t}^{\tau=2\Delta t} N_3(\tau).N_2(t_{máx}-\tau)d\tau & \int_{\tau=\Delta t}^{\tau=2\Delta t} N_3(\tau).N_3(t_{máx}-\tau)d\tau \end{bmatrix}_{3x3} . \begin{bmatrix} h_1 \\ h_2 \\ h_3 \end{bmatrix}_{3x1} \right\} .\Delta t \quad (21)$$

Solving numerically the integral expressions in Eq. (17):

$$c_2 = \left\{ \begin{bmatrix} f_1 \\ f_2 \\ f_3 \end{bmatrix}_{3x1}^T . \begin{bmatrix} \left(-\frac{4}{120}\right) & \left(-\frac{7}{120}\right) & \left(\frac{1}{120}\right) \\ \left(\frac{23}{120}\right) & \left(\frac{64}{120}\right) & \left(-\frac{7}{120}\right) \\ \left(\frac{31}{120}\right) & \left(\frac{23}{120}\right) & \left(-\frac{4}{120}\right) \end{bmatrix}_{3x3} . \begin{bmatrix} h_1 \\ h_2 \\ h_3 \end{bmatrix}_{3x1} \right\} .\Delta t \quad (22)$$

Therefore, substituting Eq. (20) and Eq. (22) into Eq. (2), results in:

$$c(t_{max}=2\Delta t) = \left\{ \begin{matrix} c_1(t_{max}=2\Delta t) = \left\{ \begin{bmatrix} f_1 \\ f_2 \\ f_3 \end{bmatrix}_{3x1}^T . \begin{bmatrix} \left(-\frac{4}{120}\right) & \left(\frac{23}{120}\right) & \left(\frac{31}{120}\right) \\ \left(-\frac{7}{120}\right) & \left(\frac{64}{120}\right) & \left(\frac{23}{120}\right) \\ \left(\frac{1}{120}\right) & \left(-\frac{7}{120}\right) & \left(-\frac{4}{120}\right) \end{bmatrix}_{3x3} . \begin{bmatrix} h_1 \\ h_2 \\ h_3 \end{bmatrix}_{3x1} \right\} + \\ \cdots\cdots\cdots\cdots\cdots\cdots\cdots\cdots\cdots\cdots\cdots\cdots \\ c_2(t_{max}=2\Delta t) = \left\{ \begin{bmatrix} f_1 \\ f_2 \\ f_3 \end{bmatrix}_{3x1}^T . \begin{bmatrix} \left(-\frac{4}{120}\right) & \left(-\frac{7}{120}\right) & \left(\frac{1}{120}\right) \\ \left(\frac{23}{120}\right) & \left(\frac{64}{120}\right) & \left(-\frac{7}{120}\right) \\ \left(\frac{31}{120}\right) & \left(\frac{23}{120}\right) & \left(-\frac{4}{120}\right) \end{bmatrix}_{3x3} . \begin{bmatrix} h_1 \\ h_2 \\ h_3 \end{bmatrix}_{3x1} \right\} \end{matrix} \right\} .\Delta t \quad (23)$$

Equation (23) can be generalized for the interval $0 \leq \tau \leq n\Delta t$ (see Eq. (26) in the next page).

5. NUMERICAL RESULTS

In this section, the numerical results of the implemented higher order convolution integrals are compared with the analytical solution of a one degree of freedom system, Fig. (6-a), excited by a harmonic force. In Eq. (24), F_0 is the amplitude of the cosine force and ω is the excitation frequency of the system.

$$F(t) = F_0 \cos(\omega t) \quad (24)$$

According to Inman (2014), the analytical response of a one-degree-of-freedom (1 DOF) mass-spring-damping system excited by a cosine force is given by the sum of a particular and a homogeneous solution, as shown in Eq. (25), and its parameters are: $\omega_n = (k/m)^{1/2}$ is the natural frequency of the system, $\xi = c/(2.(k.m)^{1/2})$ is the damping factor, and $\omega_d = \omega_n.(1-\xi^2)^{1/2}$ is the cushioned frequency of the system.

$$u(t)_{analytical} = A_m e^{(-\xi\omega_n t)} sen(\omega_d t + \varphi) + X_m \cos(\omega t - \theta) \quad (25)$$

$$c(t_{max} = n\Delta t) = \sum_{i=1}^{n} \left\{ \begin{array}{l} \text{if n is odd} \\ \left\{ \begin{bmatrix} f_{(i)} & f_{(i+1)} & f_{(i+2)} \end{bmatrix}_{1x3} . \begin{bmatrix} \left(\frac{11}{120}\right) & \left(\frac{43}{120}\right) & \left(-\frac{4}{120}\right) \\ \left(\frac{43}{120}\right) & \left(\frac{44}{120}\right) & \left(-\frac{7}{120}\right) \\ \left(-\frac{4}{120}\right) & \left(-\frac{7}{120}\right) & \left(\frac{1}{120}\right) \end{bmatrix}_{3x3} . \begin{bmatrix} h_{((n-i)+1)} \\ h_{((n-i)+2)} \\ h_{((n-i)+3)} \end{bmatrix}_{3x1} \right\}, \text{ if i is odd} \\ \text{or} \\ \left\{ \begin{bmatrix} f_{(i-1)} & f_{(i)} & f_{(i+1)} \end{bmatrix}_{1x3} . \begin{bmatrix} \left(\frac{1}{120}\right) & \left(-\frac{7}{120}\right) & \left(-\frac{4}{120}\right) \\ \left(-\frac{7}{120}\right) & \left(\frac{44}{120}\right) & \left(\frac{43}{120}\right) \\ \left(-\frac{4}{120}\right) & \left(\frac{43}{120}\right) & \left(\frac{11}{120}\right) \end{bmatrix}_{3x3} . \begin{bmatrix} h_{((n-i))} \\ h_{((n-i)+1)} \\ h_{((n-i)+2)} \end{bmatrix}_{3x1} \right\}, \text{ if i is even} \\ \cdots\cdots\cdots\cdots\cdots\cdots\cdots\cdots\cdots\cdots\cdots\cdots \\ \text{If n is even} \\ \left\{ \begin{bmatrix} f_{(i)} & f_{(i+1)} & f_{(i+2)} \end{bmatrix}_{1x3} . \begin{bmatrix} \left(-\frac{4}{120}\right) & \left(\frac{23}{120}\right) & \left(\frac{31}{120}\right) \\ \left(-\frac{7}{120}\right) & \left(\frac{64}{120}\right) & \left(\frac{23}{120}\right) \\ \left(\frac{1}{120}\right) & \left(-\frac{7}{120}\right) & \left(-\frac{4}{120}\right) \end{bmatrix}_{3x3} . \begin{bmatrix} h_{((n-i))} \\ h_{((n-i)+1)} \\ h_{((n-i)+2)} \end{bmatrix}_{3x1} \right\}, \text{ if i is odd} \\ \text{or} \\ \left\{ \begin{bmatrix} f_{(i-1)} & f_{(i)} & f_{(i+1)} \end{bmatrix}_{1x3} . \begin{bmatrix} \left(-\frac{4}{120}\right) & \left(-\frac{7}{120}\right) & \left(\frac{1}{120}\right) \\ \left(\frac{23}{120}\right) & \left(\frac{64}{120}\right) & \left(-\frac{7}{120}\right) \\ \left(\frac{31}{120}\right) & \left(\frac{23}{120}\right) & \left(-\frac{4}{120}\right) \end{bmatrix}_{3x3} . \begin{bmatrix} h_{((n-(i-2))-1)} \\ h_{((n-(i-2)))} \\ h_{((n-(i-2))+1)} \end{bmatrix}_{3x1} \right\}, \text{ if i is even} \end{array} \right\} .\Delta t \qquad (26)$$

According to Inman (2014), the analytical response of a 1 DOF mass-spring-damping system excited by a unit pulse, is given by Eq. (27), $\hat{F}$ is the amplitude of the impulse force.

$$u(t)_{impulse} = \left(\frac{\hat{F}e^{-\xi\omega_n t}}{m\ \omega_d} \right).\sin\left(\omega_d t\right) \qquad (27)$$

Substituting Eqs. (25) and (27) into Eq. (1), one can obtain the expression for the convolution integral:

$$c(t_{max}) = \int_{\tau=0}^{\tau=t_{max}} \left[F_0 \cos\left(\omega\tau\right) \right] . \left[\left(\frac{\hat{F}e^{-\xi\omega_n\left(t_{max}-\tau\right)}}{m\ \omega_d} \right).\sin\left(\omega_d\left(t_{max}-\tau\right)\right) \right] d\,\tau \qquad (28)$$

Figure (6-a) presents the dynamic system model used in the problem, and Fig. (6-b) presents the analytical and numerical solution for displacement of the 1 DOF mass-spring-damping system, for the case in which m=30kg, k=15N/m, c=15N.s/m. In Fig. (6-b), the abbreviation ‘T.I’ in the legend means time interpolation.

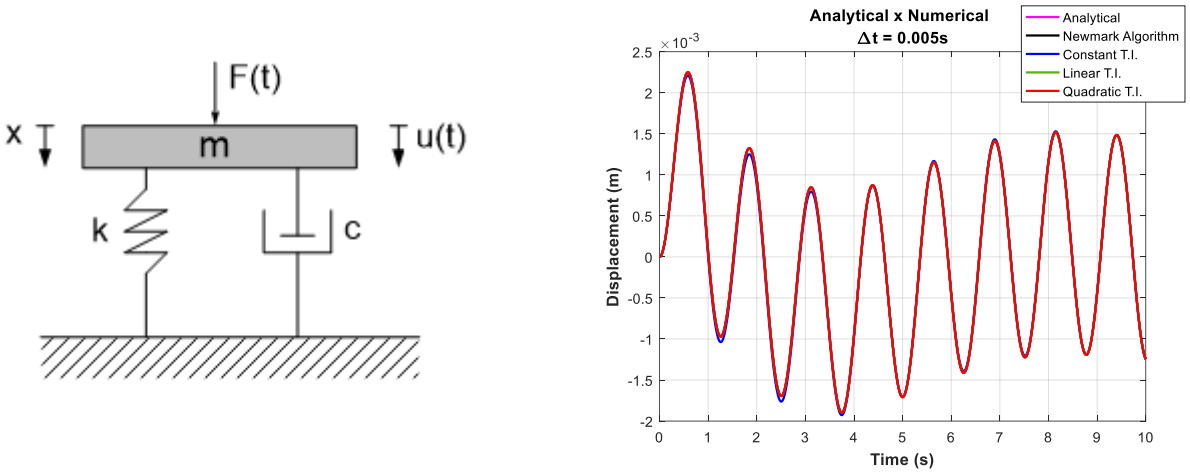

(a) (b)

Figure 6. (a) 1 DOF mass-spring-damping system. (b) Displacement of dynamic system.

Figure (7-a) presents the absolute error between analytical and numerical solution and Fig. (7-b) presents the relative error between analytical and numerical solution. In this work, absolute and relative errors are defined by Eqs. (29) and (30), respectively. The terms $u_{analytical}$ and $u_{numerical}$ described in Eqs. (29) and (30) are the displacements of the system obtained through analytical and numerical method.

$$error_{absolute} = \left| u_{analytical} - u_{numerical} \right| \tag{29}$$

$$error_{relative} = \left| \frac{u_{analytical} - u_{numerical}}{u_{analytical}} \right| \tag{30}$$

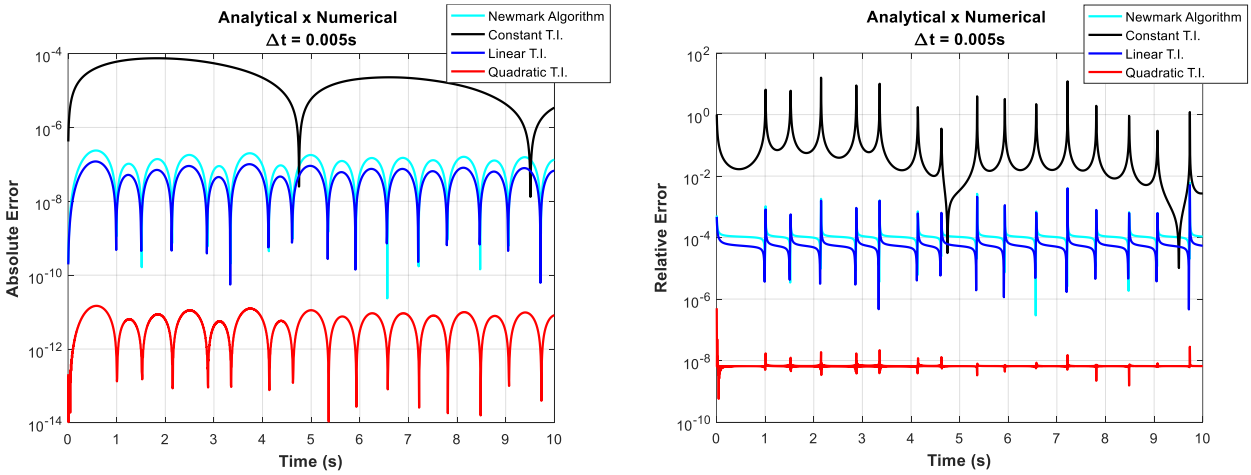

(a) (b)

Figure 7. Comparison between analytical and numerical solution. (a) Absolute error. (b) Relative error.

Figure (8-a) presents the convergence of absolute error between analytical and numerical solution. Fig. (8-b) presents the convergence of relative error between analytical and numerical solution.

Figure (8) shows that the numerical convolution integral proposed in this paper provides a better approximation of the analytical solution than Newmark integration procedure. The convergence rate for both the Newmark Algorithm and the Linear Time Interpolation scheme is 2, while this rate is 1 for the Constant Time Interpolation and 4 for the Quadratic Time Interpolation schemes.

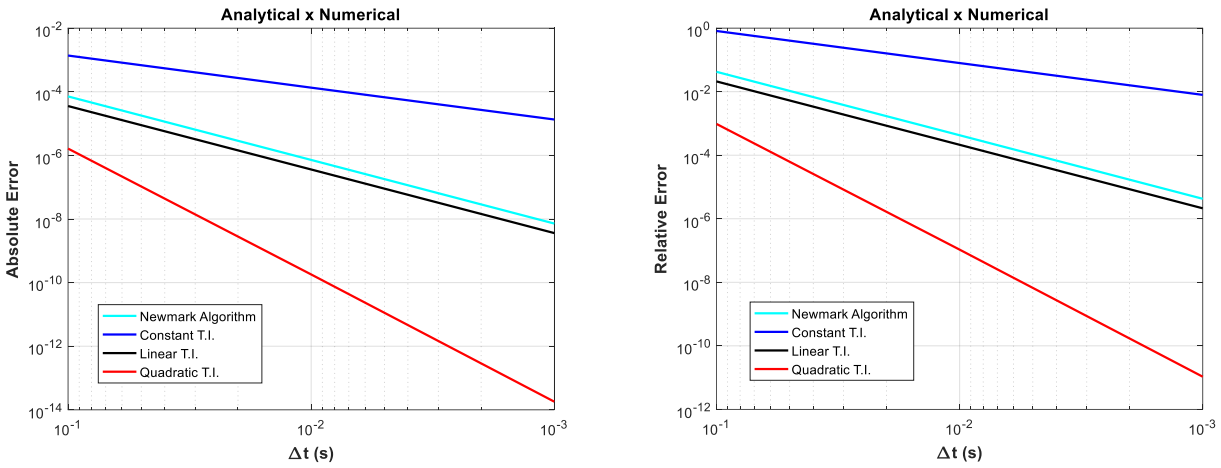

Figure 8. Convergence of error between analytical and numerical solution. (a) Absolut error. (b) Relative error

6. CONCLUSIONS

This article presented the formulation for higher order Duhamel´s convolution integrals and their numerical implementation schemes. The solution of a representative one-degree-of-freedom mass-spring-damping system through the proposed numerical convolution integral approximated by second order shape functions is significantly better than the numerical solution by Newmark Method. The convergence rate of absolute and relative errors for the second order approximation for the convolution integral is twice that of the numerical approximation using Newmark Method.

This new formulation for the numerical convolution integral will be essential to improve the quality and accuracy of the iterative coupling scheme for soil-structure interaction problems based on the Newmark and convolution integral.

7. ACKNOWLEDGEMENTS

The research leading to this work has been funded by the São Paulo Research Foudation (Fapesp) through grants 2012/17948-4 and 2017/01450-0, and FAPESP CEPID Process 2013/08293-7. The support of Capes, CNPq and Faepex/Unicamp is also gratefully acknowledged.

8. REFERENCES

Carrion, R., Souza, A.D.O., Mesquita, E., 2007, “The influence of soil damping mechanisms and geo-profiles on the stationary response of 3D rigid block foundations”, Proceedings of the 19th Brazilian Congress of Mechanical Engineering, Brasília, DF, Brazil.

Cheng, D.K., 1972, “Analysis of Linear Systems”, 3th ed, Ed. Addison-Wesley, Massachusetts, EUA, 431p.

Coda, H.B., Venturini, W.S., 1995, “Non-singular time-steping BEM for transient elastodynamic analysis”, Engineering Analysis with Boundary Elements, Vol.15, pp. 11-15.

Damasceno, D.A., 2013, “Transient Analysis of Systems with Soil-Structure Interaction through Iterative Coupling Techniques”, Master thesis, University of Campinas, Brazil.

Damasceno, D.A., Labaki, J., Mesquita, E., 2013, “Dynamic Transient Analysis of Partitioned Systems Through an Interative Coupling Technique”, Proceedings of the XXXIV Iberian Latin-American Congress on Computational Methods in Engineering, Pirenópolis, GO, Brazil, pp. 01-20.

Gaul, D.A., Schanz, M., Fiedler, C., 1992, “Viscoelastic formulations of BEM in time and frequency domain”, Engineering Analysis with Boundary Elements, vol.10, pp. 137-141.

Inman, D.J., 2014, “Engineering Vibration”, 4th ed., Ed. Pearson, Boston, Massachusetts, EUA, 707 p.

Labaki, J., Mesquita, E., Rajapakse, R.K.N.D., 2014, “Vertical Vibrations of an Elastic Foundation with Arbitrary Embedment within a Transversely Isotropic, Layered Soil”, CMES: Computer Modeling in Engineering & Sciences, Vol. 103, No. 5, pp. 281-313.

Mesquita, E., Antes, H., Thomazo, L.H., Adolph, M., 2012, “Transient wave propagation phenomena at visco-elastic half-spaces under distributed surface loadings”, Latin American Journal of Solids and Structures, Vol. 9, No. 4, pp. 453-474.

9. RESPONSIBILITY NOTICE

The authors are the only responsible for the printed material included in this paper.